Development of a two-particle self-consistent method for multi-orbital systems and its application to unconventional superconductors

Hideyuki Miyahara[1], Ryotaro Arita[1,2], and Hiroaki Ikeda[3]

[1]*Department of Applied Physics, University of Tokyo,*
7-3-1 Hongo, Bunkyo-ku, Tokyo, 113-8656, Japan
[2]*JST PRESTO, Kawaguchi, Saitama, 332-0012, Japan and*
[3]*Department of Physics, Kyoto University, Kyoto 606-8502, Japan*
(Dated: January 16, 2013)

We extend the two-particle self-consistent method proposed by Vilk and Tremblay (J. Phys. I France 7, 1309-1368 (1997)) to study superconductivity in multi-orbital systems. Starting with the sum rules for the spin and charge susceptibilities, we derive self-consistent equations to determine the renormalized effective interactions. We apply this method to the two-orbital $d_{x^2-y^2}$-$d_{3z^2-r^2}$ model for La_2CuO_4 and the five-orbital d-model for LaFeAsO. Comparing the results with those of the random phase approximation or the fluctuation exchange approximation in which vertex corrections are ignored, we discuss how the vertex corrections affect the pairing instability of La_2CuO_4 and the dominant pairing symmetry of LaFeAsO.

I. INTRODUCTION

Since the seminal studies by Suhl[1] and Kondo,[2] superconductivity in multi-orbital systems has been one of the major topics in condensed matter physics. So far, many kinds of multi-orbital superconductors such as MgB_2 (Ref. 3), alkali-doped C_{60} (Ref. 4), $Na_xCoO_2 \cdot yH_2O$ (Ref. 5), Sr_2RuO_4 (Ref. 6), iron-based superconductors,[7] and heavy fermion superconductors[8] have been discovered and studied extensively. Theoretically, a variety of exotic unconventional pairing mechanisms going beyond the Migdal-Eliashberg theory[9] have been proposed. For example, it has been considered for the cobaltate superconductor that the Hund's coupling (which of course does not exist for single-orbital systems) induces triplet superconductivity,[10] and it has recently become an issue of hot debates whether orbital fluctuations mediate superconductivity in the iron-based superconductors.[11]

To investigate these fascinating possibilities, accurate calculations of superconductivity in correlated multi-orbital models are indispensable. Among many available approaches, from the weak coupling side, one often starts with the random phase approximation (RPA). Since the pioneering work for the single-band Hubbard model by Scalapino *et al.*,[12] RPA has been successfully applied to various multi-orbital systems. The fluctuation exchange approximation (FLEX) developed by Bickers *et al.*,[13] which includes the self-energy correction self-consistently, has been also widely used. Here, the self-energy is calculated in the manner of Baym and Kadanoff,[14] and conservation laws for one-particle quantities such as the total energy and momentum are satisfied. However, due to the absence of vertex corrections, FLEX violates conservation laws for two-particle quantities.

Recently, several diagrammatic methods, which take into account some vertex corrections, have been proposed.[15,16] Among them, the two-particle self-consistent method (TPSC) proposed by Vilk and Tremblay[17] is a promising approach in that it is compatible with conservation laws in the two-particle level.

In this method, vertex corrections in the charge and spin channel are assumed to be momentum and frequency independent, and they are determined in such a way that the correlation functions meet their sum rules. With this numerically inexpensive treatment, it has been demonstrated for the single-band Hubbard model that TPSC shows good agreement with quantum Monte Carlo (QMC) calculations.

In this paper, we formulate TPSC for the multi-orbital Hubbard model. First, we derive a series of equations to determine the vertex corrections in the spin and charge channel, and then apply this method to a two-orbital model for $La_{2-x}(Sr/Ba)_xCuO_4$ and a five-orbital model for F-doped LaFeAsO. Recently, the two-orbital model (which we call the $d_{x^2-y^2}$-$d_{3z^2-r^2}$ model) was studied by FLEX[18] to give an insight into the material dependence of superconducting transition temperature (T_c). While FLEX successfully describes the difference between $La_{2-x}(Sr/Ba)_xCuO_4$ ($T_c \sim 40$ K) and $HgBa_2CuO_{4+\delta}$ ($T_c \sim 90$ K), it underestimates the pairing instability for $La_{2-x}(Sr/Ba)_xCuO_4$ and T_c is much lower than the experimental value. We show that, in the present multi-orbital TPSC calculation, the inter-orbital scattering enhances the d-wave instability and reasonable value of T_c is obtained for the intermediate coupling regime. For the five-orbital model, it has been extensively studied by RPA[19,20,22] and FLEX.[21] There, strong spin fluctuation has been shown to mediate the s-wave superconductivity with sign changes (the so-called $s_\pm$-wave pairing). On the other hand, recently, it has been pointed out that vertex corrections can enhance orbital fluctuations, which mediate s-wave superconductivity without sign changes (the s_{++}-wave pairing).[16] In this paper, we show that orbital fluctuations are enhanced in TPSC, while the dominant pairing symmetry is still $s_\pm$ when the system resides in the weak coupling regime.

This paper is organized as follows. In Sec. II, we formulate multi-orbital TPSC for the Hubbard model. We discuss how we calculate the charge (orbital) and spin correlation functions. In Sec. III, we show the results for

the two- and five-orbital Hubbard model and the summary of the present study is given in Sec. IV.

II. METHOD

A. Model

The Hamiltonian of the multi-orbital Hubbard model is given by

$$H = \sum_{\mathbf{r}\mu\sigma} \epsilon_\mu n_{\mu\sigma}(\mathbf{r}) + \sum_{\mathbf{r}\mathbf{r}'\mu\nu\sigma} t_{\mathbf{r}\mathbf{r}'}^{\mu\nu} c_{\mu\sigma}^\dagger(\mathbf{r}) c_{\nu\sigma}(\mathbf{r}')$$
$$+ \sum_{\mathbf{r}} \Big[U \sum_\mu n_{\mu\uparrow}(\mathbf{r}) n_{\mu\downarrow}(\mathbf{r}) + U' \sum_{\mu>\nu} \sum_{\sigma\sigma'} n_{\mu\sigma}(\mathbf{r}) n_{\nu\sigma'}(\mathbf{r})$$
$$- J \sum_{\mu\neq\nu} \mathbf{S}_\mu(\mathbf{r}) \cdot \mathbf{S}_\nu(\mathbf{r}) + J' \sum_{\mu\neq\nu} c_{\mu\uparrow}^\dagger(\mathbf{r}) c_{\mu\downarrow}^\dagger(\mathbf{r}) c_{\nu\downarrow}(\mathbf{r}) c_{\nu\uparrow}(\mathbf{r}) \Big],$$

where $c_{\mu\sigma}^\dagger(\mathbf{r})$ is a creation operator of an electron with spin σ and orbital μ at site $\mathbf{r}$, and $n_{\mu\sigma}(\mathbf{r}) = c_{\mu\sigma}^\dagger(\mathbf{r}) c_{\mu\sigma}(\mathbf{r})$, $\mathbf{S}_\mu(\mathbf{r}) = (c_{\mu\uparrow}^\dagger(\mathbf{r}), c_{\mu\downarrow}^\dagger(\mathbf{r})) \, \boldsymbol{\sigma} \, (c_{\mu\uparrow}(\mathbf{r}), c_{\mu\downarrow}(\mathbf{r}))^T$ with the Pauli matrices $\boldsymbol{\sigma}$. The on-site Coulomb interactions, U, U', J, J' denote the intra-orbital, inter-orbital Coulomb repulsions, the Hund's exchange, and the pair-hopping term, respectively.

B. Two-particle self-consistent method for the single-orbital Hubbard model

Let us start with a review of TPSC for the single-orbital Hubbard model formulated by Vilk and Tremblay.[17] The central quantities in this method are the spin and charge correlation functions. In the non-magnetic state, the system holds SU(2) symmetry, and the spin-spin correlation functions do not depend on the spin directions. Thus we consider the z component of the spin operator $S^z(\mathbf{r}) = n_\uparrow(\mathbf{r}) - n_\downarrow(\mathbf{r})$ and the charge operator $n(\mathbf{r}) = n_\uparrow(\mathbf{r}) + n_\downarrow(\mathbf{r})$. In RPA, the spin and charge correlation functions are evaluated as follows:

$$\chi_{\mathrm{RPA}}^{\mathrm{sp}}(q) = \frac{2\chi^0(q)}{1 - U\chi^0(q)}, \quad \chi_{\mathrm{RPA}}^{\mathrm{ch}}(q) = \frac{2\chi^0(q)}{1 + U\chi^0(q)}, \quad (1)$$

with the irreducible susceptibility,

$$\chi^0(q) = -\frac{T}{N} \sum_k G^0(k) G^0(k+q),$$

where T and N are temperature and number of sites in the system, and $G^0(k) = 1/(i\epsilon_n + \mu - \epsilon(\mathbf{k}))$ is the bare Green's function with chemical potential μ and energy dispersion $\epsilon(\mathbf{k})$. Here, we have introduced the abbreviations $k = (\mathbf{k}, i\epsilon_n)$ and $q = (\mathbf{q}, i\nu_n)$ being the fermionic and bosonic Matsubara frequencies, respectively.

Note that the RPA violates the Pauli principles, and it does not fulfill the following two sum rules,

$$\frac{T}{N} \sum_q \chi^{\mathrm{sp}}(q) = \langle (n_\uparrow(\mathbf{r}) - n_\downarrow(\mathbf{r}))(n_\uparrow(\mathbf{r}) - n_\downarrow(\mathbf{r})) \rangle$$
$$= n - 2\langle n_\uparrow n_\downarrow \rangle, \quad (2a)$$
$$\frac{T}{N} \sum_q \chi^{\mathrm{ch}}(q) = \langle (n_\uparrow(\mathbf{r}) + n_\downarrow(\mathbf{r}))(n_\uparrow(\mathbf{r}) + n_\downarrow(\mathbf{r})) \rangle - n^2$$
$$= n + 2\langle n_\uparrow n_\downarrow \rangle - n^2, \quad (2b)$$

which are exact relations derived via the Pauli principles, $\langle n_\sigma(\mathbf{r})^2 \rangle = \langle n_\sigma(\mathbf{r}) \rangle$ (see Appendix A). Here, n is the particle number per site and for nonmagnetic states, $\langle n_\uparrow(\mathbf{r}) \rangle = \langle n_\downarrow(\mathbf{r}) \rangle = n/2$. Note that the double occupancy, $\langle n_\uparrow(\mathbf{r}) n_\downarrow(\mathbf{r}) \rangle \equiv \langle n_\uparrow n_\downarrow \rangle$ is also translation invariant and does not depend on site $\mathbf{r}$.

In TPSC, to meet the above conditions [Eqs. (2)], we introduce two independent effective interactions, U^{sp} for the spin channel and U^{ch} for the charge channel. Then the full susceptibilities of Eq. (1) are replaced with

$$\chi^{\mathrm{sp}}(q) = \frac{2\chi^0(q)}{1 - U^{\mathrm{sp}}\chi^0(q)}, \quad \chi^{\mathrm{ch}}(q) = \frac{2\chi^0(q)}{1 + U^{\mathrm{ch}}\chi^0(q)}. \quad (3)$$

Finally, we put the following ansatz:

$$U^{\mathrm{sp}} = \frac{\langle n_\uparrow n_\downarrow \rangle}{\langle n_\uparrow \rangle \langle n_\downarrow \rangle} U, \quad (4)$$

which is compatible with the equations of motion (see Appendix B). Equations (2), (3), and (4) provide a set of self-consistent equations in TPSC. Namely, U^{ch}, U^{sp}, and $\langle n_\uparrow n_\downarrow \rangle$ are self-consistently determined for given n and U. The one-particle Green's function and self-energy are calculated by

$$G(k) = G^0(k) + G^0(k)\Sigma(k)G(k),$$
$$\Sigma(k) = \frac{1}{4}\frac{T}{N} \sum_q \Big[U^{\mathrm{sp}}\chi^{\mathrm{sp}}(q)U + U^{\mathrm{ch}}\chi^{\mathrm{ch}}(q)U \Big] G(k-q).$$

For the single-band Hubbard model, it has been demonstrated that TPSC agrees well with QMC.[17]

C. Extension to multi-orbital systems

Let us here formulate TPSC for the multi-orbital Hubbard model. Hereafter, we follow the matrix form employed in Refs. 10 and 23. The irreducible susceptibility is defined as

$$\chi_{\lambda\mu\nu\xi}^0(q) = -\frac{T}{N} \sum_k G_{\nu\lambda}^0(k) G_{\mu\xi}^0(k+q), \quad (5)$$

which can be considered as a matrix element with a row $\lambda\mu$ and a column $\nu\xi$ of a matrix $\boldsymbol{\chi}^0(q)$. In the non-magnetic state, the system is invariant for spin rotation, and then $2\boldsymbol{\chi}^{\mathrm{sp}z}(q) = \boldsymbol{\chi}^{\mathrm{sp}\pm}(q)$ holds, where $\boldsymbol{\chi}^{\mathrm{sp}\pm}(q)$

is the in-plane correlation function between $S_{\lambda\mu}^{\pm}(\mathbf{r}) = S_{\lambda\mu}^{x}(\mathbf{r}) \pm iS_{\lambda\mu}^{y}(\mathbf{r}) = c_{\lambda\sigma}^{\dagger}(\mathbf{r})c_{\mu\bar{\sigma}}(\mathbf{r})$ with $\sigma = \uparrow$ or $\downarrow$. In TPSC, similar to the single-orbital case, the spin and charge susceptibilities are given by

$$\boldsymbol{\chi}^{\mathrm{sp}}(q) = (\mathbf{1} - \boldsymbol{\chi}^{0}(q)\mathbf{U}^{\mathrm{sp}})^{-1}2\boldsymbol{\chi}^{0}(q), \tag{6a}$$

$$\boldsymbol{\chi}^{\mathrm{ch}}(q) = (\mathbf{1} + \boldsymbol{\chi}^{0}(q)\mathbf{U}^{\mathrm{ch}})^{-1}2\boldsymbol{\chi}^{0}(q), \tag{6b}$$

where $\mathbf{U}^{\mathrm{sp(ch)}}$ is the renormalized effective interaction matrix for the spin (charge) channel.[10,23] For two-orbital systems, for instance, these are represented as

$$\mathbf{U}^{\mathrm{sp}} = \begin{pmatrix} U_{1111}^{\mathrm{sp}} & J^{\mathrm{sp}} & 0 & 0 \\ J^{\mathrm{sp}} & U_{2222}^{\mathrm{sp}} & 0 & 0 \\ 0 & 0 & U_{1212}^{\mathrm{sp}} & J^{\mathrm{sp}} \\ 0 & 0 & J^{\mathrm{sp}} & U_{2121}^{\mathrm{sp}} \end{pmatrix}, \tag{7a}$$

$$\mathbf{U}^{\mathrm{ch}} = \begin{pmatrix} U_{1111}^{\mathrm{ch}} & 2U_{1122}^{\mathrm{ch}} - J^{\mathrm{ch}} & 0 & 0 \\ 2U_{2211}^{\mathrm{ch}} - J^{\mathrm{ch}} & U_{2222}^{\mathrm{ch}} & 0 & 0 \\ 0 & 0 & -U_{1212}^{\mathrm{ch}} + 2J^{\mathrm{ch}} & 0 \\ 0 & 0 & 0 & -U_{2121}^{\mathrm{ch}} + 2J^{\mathrm{ch}} \end{pmatrix}, \tag{7b}$$

where $U_{\mu\mu\mu\mu}^{\mathrm{sp}}$ ($U_{\mu\mu\mu\mu}^{\mathrm{ch}}$) is the intra-orbital Coulomb interaction; $U_{\mu\nu\mu\nu}^{\mathrm{sp}}$ ($U_{\mu\nu\mu\nu}^{\mathrm{ch}}$) with $\mu \neq \nu$, the inter-orbital Coulomb interaction; J^{sp} (J^{ch}), the Hund's coupling.[10,23] In the present study, for simplicity, we ignore the Hund's coupling in the charge channel, namely, $J^{\mathrm{ch}} = 0$.[24] In RPA, one employs the unperturbed bare vertex as follows, $U_{\mu\mu\mu\mu}^{\mathrm{sp(ch)}} = U$, $U_{\mu\mu\nu\nu}^{\mathrm{sp(ch)}} = U_{\mu\nu\mu\nu}^{\mathrm{sp(ch)}} = U'$, and $J^{\mathrm{sp(ch)}} = J$.

Next let us consider the sum rule for multi-orbital systems (see Appendix A). In the n-orbital Hubbard model, there are n^4 sum rules for $\boldsymbol{\chi}^{\mathrm{sp}}(q)$ and $\boldsymbol{\chi}^{\mathrm{ch}}(q)$. Among them, we use the following equations to determine $\mathbf{U}^{\mathrm{sp}}$:

$$\frac{T}{N}\sum_{q}\chi_{\mu\mu\mu\mu}^{\mathrm{spz}}(q) = 2\langle n_{\mu\uparrow}\rangle - 2\langle n_{\mu\uparrow}n_{\mu\downarrow}\rangle, \tag{8a}$$

$$\frac{T}{N}\sum_{q}\chi_{\mu\nu\mu\nu}^{\mathrm{sp\pm}}(q) = 2\langle c_{\mu\uparrow}^{\dagger}c_{\nu\downarrow}c_{\nu\downarrow}^{\dagger}c_{\mu\uparrow}\rangle$$

$$= 2\langle n_{\mu\uparrow}\rangle - 2\langle n_{\mu\uparrow}n_{\nu\downarrow}\rangle, \tag{8b}$$

$$\frac{T}{N}\sum_{q}\chi_{\mu\mu\nu\nu}^{z\pm}(q) = 2\langle n_{\mu\uparrow}n_{\nu\uparrow}\rangle - 2\langle n_{\mu\uparrow}n_{\mu\downarrow}\rangle. \tag{8c}$$

Note that the intra-orbital component of the sum rule has the same form as that of the single-orbital Hubbard model. For the inter-orbital components, we use $\boldsymbol{\chi}^{\mathrm{sp\pm}}(q)$ rather than $\boldsymbol{\chi}^{\mathrm{spz}}(q)$, since they can be expressed in terms of the density operators.

For $\mathbf{U}^{\mathrm{ch}}$, we use the following sum rules for the charge susceptibilities which can be represented by the spin sus-

ceptibilities and the double occupancy:

$$\frac{T}{N}\sum_{q}\chi_{\mu\mu\mu\mu}^{\mathrm{ch}}(q) = \langle(n_{\mu\uparrow} + n_{\mu\downarrow})(n_{\mu\uparrow} + n_{\mu\downarrow})\rangle - \langle n_{\mu}\rangle\langle n_{\mu}\rangle,$$

$$= n_{\mu} + 2\langle n_{\mu\uparrow}n_{\mu\downarrow}\rangle - n_{\mu}^{2} \tag{9a}$$

$$\frac{T}{N}\sum_{q}\chi_{\mu\nu\mu\nu}^{\mathrm{ch}}(q) = \langle(c_{\mu\uparrow}^{\dagger}c_{\nu\uparrow} + c_{\mu\downarrow}^{\dagger}c_{\nu\downarrow})(c_{\nu\uparrow}^{\dagger}c_{\mu\uparrow} + c_{\nu\downarrow}^{\dagger}c_{\mu\downarrow})\rangle$$

$$= \langle n_{\mu\uparrow}(1 - n_{\nu\uparrow})\rangle + \langle n_{\mu\downarrow}(1 - n_{\nu\downarrow})\rangle$$

$$+ \langle c_{\mu\downarrow}^{\dagger}c_{\nu\downarrow}c_{\nu\uparrow}^{\dagger}c_{\mu\uparrow}\rangle + \langle c_{\mu\uparrow}^{\dagger}c_{\nu\uparrow}c_{\nu\downarrow}^{\dagger}c_{\mu\downarrow}\rangle$$

$$= \frac{T}{N}\left(\sum_{q}\chi_{\mu\nu\mu\nu}^{\mathrm{spz}}(q) + 2\chi_{\mu\mu\nu\nu}^{\mathrm{spz}}(q)\right). \tag{9b}$$

Finally, as in the single-band case, we introduce the following ansatz between the two-particle quantities and the interaction parameters (see Appendix C);

$$U_{\mu\mu\mu\mu}^{\mathrm{sp}} = \frac{\langle n_{\sigma\mu}n_{\bar{\sigma}\mu}\rangle}{\langle n_{\sigma\mu}\rangle\langle n_{\bar{\sigma}\mu}\rangle}U, \tag{10a}$$

$$U_{\mu\nu\mu\nu}^{\mathrm{sp}} = \frac{\langle n_{\sigma\mu}n_{\bar{\sigma}\nu}\rangle}{\langle n_{\sigma\mu}\rangle\langle n_{\bar{\sigma}\nu}\rangle}U', \tag{10b}$$

$$U_{\mu\nu\mu\nu}^{\mathrm{sp}} - J^{\mathrm{sp}} = \frac{\langle n_{\sigma\mu}n_{\sigma\nu}\rangle}{\langle n_{\sigma\mu}\rangle\langle n_{\sigma\nu}\rangle}(U' - J). \tag{10c}$$

Equations. (6)-(10) are a set of self-consistent equations in the multi-orbital case.

D. Eliashberg equation

Superconductivity has been studied by the following linearized Eliashberg equation,

$$\lambda\Delta_{ll'}(k) = \sum_{k',m_i}V_{lm_1m_4l'}(k,k')G_{m_1m_2}(k')$$

$$\times \Delta_{m_2m_3}(k')G_{m_4m_3}(-k'). \tag{11}$$

Eigenstate $\Delta_{ll'}(k)$ with the largest eigenvalue λ was numerically evaluated by the power method. The superconducting transition occurs at the temperature for which λ becomes unity. Here, $G_{ll'}(k)$ is the dressed Green's function,

$$G_{ll'}(k) = G_{ll'}^{0}(k) + G_{lm}^{0}(k)\Sigma_{mm'}(k)G_{m'l'}(k), \tag{12}$$

and the self-energy $\Sigma_{ll'}(k)$ is given by

$$\Sigma_{ll'}(k) = \frac{1}{4}\frac{T}{N}\sum_{q}\Big[\mathbf{U}^{\mathrm{sp}}\boldsymbol{\chi}^{\mathrm{sp}}(q)\mathbf{U}_{0}^{\mathrm{sp}}$$

$$+ \mathbf{U}^{\mathrm{ch}}\boldsymbol{\chi}^{\mathrm{ch}}(q)\mathbf{U}_{0}^{\mathrm{ch}}\Big]_{lml'm'}G_{mm'}(k-q). \tag{13}$$

In the present study, we omit the Hartree-Fock term, since a part of its contribution is already considered in the one-body part of the Hamiltonian, which is derived from density functional calculation.

The effective interaction $V_{ll'mm'}(k, k')$ for the spin-singlet pairing can be expressed in a matrix form as follows:

$$\mathbf{V}(k) = -\frac{3}{2}\mathbf{U}^{\mathrm{sp}}\boldsymbol{\chi}^{\mathrm{sp}}(k)\ \mathbf{U}^{\mathrm{sp}}_0 + \frac{1}{2}\mathbf{U}^{\mathrm{ch}}\boldsymbol{\chi}^{\mathrm{ch}}(k)\mathbf{U}^{\mathrm{ch}}_0$$
$$-\frac{1}{2}\mathbf{U}^{\mathrm{sp}}_0 - \frac{1}{2}\mathbf{U}^{\mathrm{ch}}_0, \quad (14)$$

where $\mathbf{U}^{\mathrm{sp}}_0$ and $\mathbf{U}^{\mathrm{ch}}_0$ are the bare vertex in the spin and charge channel, respectively.[10,23]

III. RESULTS

Let us move on to the application of the multi-orbital TPSC method to the effective models for La_2CuO_4 and $LaFeAsO$. Using the technique of the maximally localized Wannier functions,[25] these models are derived from first-principles calculations. In the density-functional calculations, we employed the exchange correlation functional proposed by Perdew *et al.*,[26] and the augmented plane wave and local orbital (APW+lo) method as implemented in the WIEN2K program.[27] We then constructed the Wannier functions for the d bands around the Fermi level, using the WIEN2Wannier (Ref. 28) and the wannier90 (Ref. 29) codes.

A. La_2CuO_4

Recently, the two-orbital $d_{x^2-y^2}$-$d_{3z^2-r^2}$ Hubbard model for the cuprates were studied to understand the material dependence of T_c by FLEX.[18] There, the energy difference between the $d_{x^2-y^2}$ orbital and the $d_{3z^2-r^2}$ orbital was found to be a key parameter to characterize La_2CuO_4 and $HgBa_2CuO_4$. Namely, in the FLEX calculation for the two-orbital model, the pairing instability is stronger in the latter. On the other hand, in the former, the eigenvalue of the Eliashberg equation within FLEX does not reach unity down to $T \sim 40$ K. The purpose of this subsection is to examine how the vertex corrections in TPSC affect the superconductivity in La_2CuO_4.

The band structure of the effective two-orbital model for La_2CuO_4 is shown in Fig. 1. We set $U = 2.0$ eV, $U' = 1.6$ eV, $J = 0.2$ eV, and $n = 2.85$. We employ 64×64 k-point meshes and 2048 Matsubara frequencies. Hereafter, orbitals 1 and 2 denote the $d_{x^2-y^2}$ and $d_{3z^2-r^2}$ orbitals, respectively.[30]

In Fig. 2, we plot temperature dependence of λ, the maximum eigenvalue of the Eliashberg equation. While λ does not show appreciable temperature dependence in FLEX, λ is drastically enhanced at low temperature < 0.02 eV in TPSC. The characteristic enhancement of λ in TPSC is attributed to the low-temperature behaviors of the spin and charge susceptibility. In Fig. 3, we plot $\chi^{\mathrm{sp}}_{1111}(\mathbf{q}, \omega = 0)$, $\chi^{\mathrm{ch}}_{1212}(\mathbf{q}, \omega = 0)$, and $-\chi^{\mathrm{ch}}_{1221}(\mathbf{q}, \omega = 0)$ at $T = 0.020$ eV, which indicate that the system has a strong incommensurate spin correlation in the $d_{x^2-y^2}$
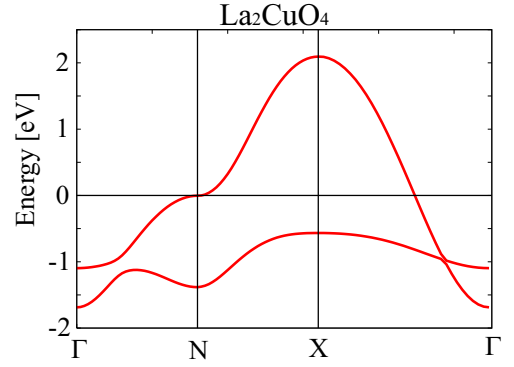

FIG. 1: (Color online) Band structure of the two-orbital model for La_2CuO_4. The model consists of the $d_{x^2-y^2}$ orbital and the $d_{3z^2-r^2}$ orbital. The Fermi level is set at 0 eV.
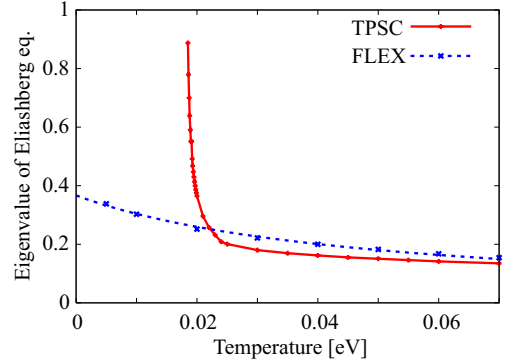

FIG. 2: (Color online) Temperature dependence of the maximum eigenvalue of the linearized Eliashberg equation obtained by TPSC (red solid line) and FLEX (blue dotted line). U and J are 2.0 eV and 0.2 eV, respectively, and n is set to be 2.85.

orbital and strong commensurate inter-orbital fluctuations. We here stress that there is no large peak in the charge susceptibilities in the RPA and FLEX calculations, so that these enhanced inter-orbital charge fluctuations are purely due to the effects of vertex corrections. It should be noted that $\chi^{\mathrm{ch}}_{1221}(Q)$ has a negative peak around $Q = (\pi, \pi)$, which works as attractive force between the two orbitals for d-wave pairing just like antiferromagnetic spin fluctuations. [Note that the spin and charge sectors in Eq. (14) have opposite signs.] As we will see below, there is a close correlation between the characteristic enhancement of λ and the charge fluctuations.

Figure 4 depicts temperature dependence of the maximum value in the spin susceptibility, the orbital susceptibility, and its inverse. We can see that the enhancement of the peaks in $\chi^{\mathrm{ch}}_{1212}$ and $-\chi^{\mathrm{ch}}_{1221}$ dominate over that of $\chi^{\mathrm{sp}}_{1111}$ for $T < 0.02$ eV. This behavior comes from the fact that while $\mathbf{U}^{\mathrm{sp}}$ is renormalized substantially ($U^{\mathrm{sp}}_{1111} \sim 1.16$ eV at $T = 0.020$ eV), $\mathbf{U}^{\mathrm{ch}}_{33}$ ($\mathbf{U}^{\mathrm{ch}}_{44}$)
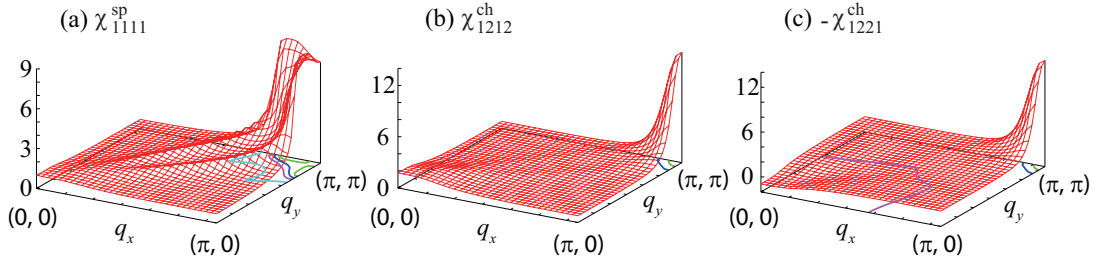
FIG. 3: (Color online) (a) $\chi^{\mathrm{sp}}_{1111}(\mathbf{q}, \omega = 0)$, (b) $\chi^{\mathrm{ch}}_{1212}(\mathbf{q}, \omega = 0)$, and (c) $-\chi^{\mathrm{ch}}_{1221}(\mathbf{q}, \omega = 0)$ at $T = 0.020$ eV, where orbitals 1 and 2 denote the $d_{x^2-y^2}$ and $d_{3z^2-r^2}$ orbitals, respectively.
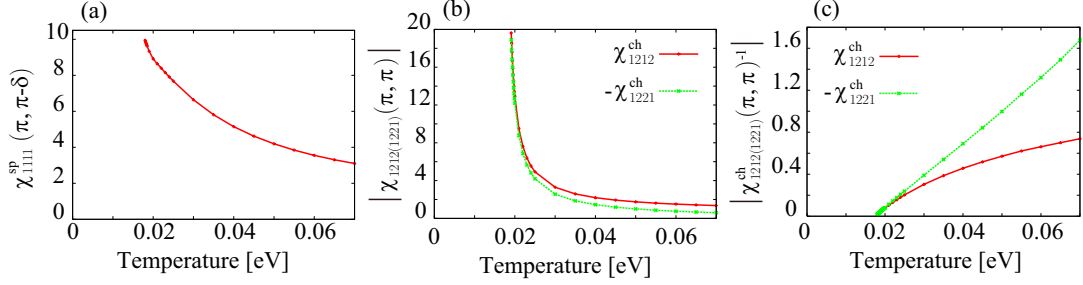

FIG. 4: (Color online) Temperature dependence of the maximum value in (a) $\chi^{\mathrm{sp}}_{1111}$, (b) $|\chi^{\mathrm{ch}}_{1212(1221)}|$, and (c) $|\chi^{\mathrm{ch}}_{1212(1221)}{}^{-1}|$.

becomes ~ 1.55 eV, which is even larger than the bare value 1.2 eV used in RPA and FLEX. In fact, similar enhancement of charge channel is also observed in the case of the single-orbital model.[17]

Figure 5 shows the gap functions for the $d_{x^2-y^2}$ orbital and the $d_{3z^2-r^2}$ orbital (Δ_{11} and Δ_{22}) at $T = 0.022$ eV. They have the d-wave symmetry, which is mediated by the dominant spin fluctuation, denoted by the black arrow. This is the conventional situation where the orbital fluctuations remains small.
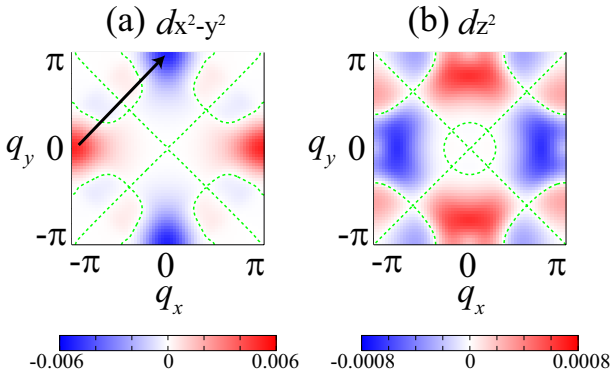
ture $T = 0.018$ eV. We see that characteristic structure emerges at $(\pi, 0)$ and $(0, \pi)$ in the $d_{3z^2-r^2}$ gap function, due to the inter-orbital effective interaction, dominantly mediated by the orbital fluctuation $\chi^{\mathrm{ch}}_{1221}(q)$, which connects Δ_{11} and Δ_{22} [Eq. (11)]. Since $\chi^{\mathrm{ch}}_{1221}(q)$ takes a large negative value around (π, π), it cooperates with antiferromagnetic spin fluctuation to enhance the d-wave pairing instability.
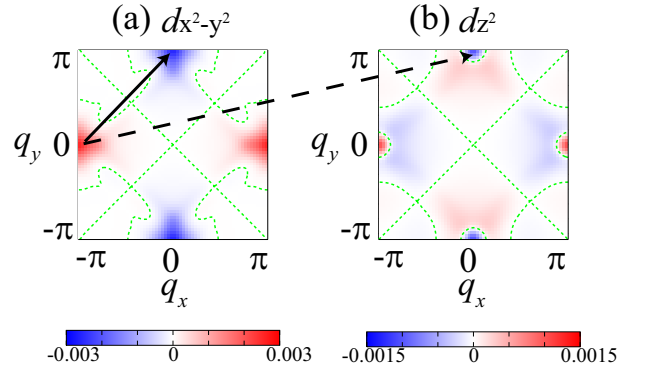

FIG. 6: (Color online) Plots similar to Fig. 5 for $T = 0.018$ eV. The dashed black arrow denotes the pair scattering mediated by orbital fluctuations.

FIG. 5: (Color online) Gap function for the (a) $d_{x^2-y^2}$ orbital and the (b) $d_{3z^2-r^2}$ orbital at $T = 0.022$ eV. The gap functions have d-wave symmetry and the black arrow denotes the pair scattering mediated by antiferromagnetic spin fluctuations.

In Fig. 6, we plot the gap functions at lower tempera-

This situation changes in the stronger coupling regime ($U \sim 2.5$ eV), where the system goes away from a superconducting instability. This is because the dominant spin/orbital fluctuations make the quasi-particle damp-
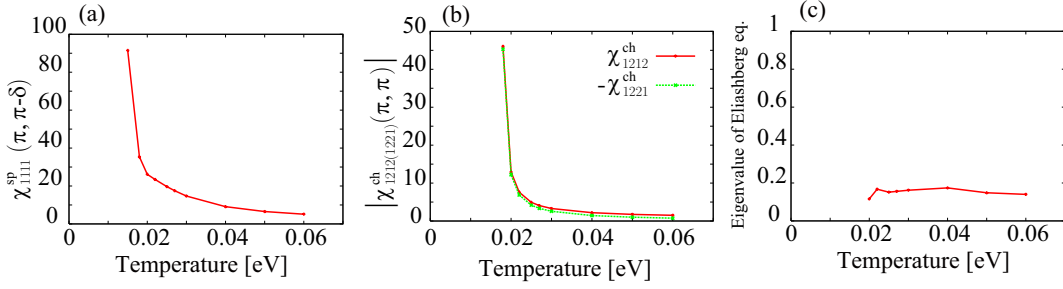
FIG. 7: (Color online) Temperature dependence of the maximum value in (a) $\chi^{\rm sp}_{1111}$, (b) $|\chi^{\rm ch}_{1212(1221)}|$, and (c) the maximum eigenvalue of the linearized Eliashberg equation obtained by TPSC for $U = 2.5$ eV, $U' = 2.0$ eV, and $J = 0.25$ eV.

ing around $(0, \pi)$ and $(\pi, 0)$ significant, as is observed in the previous FLEX calculation.[18] Temperature dependence of the maximum value in the spin, orbital susceptibility and the maximum eigenvalue of the Eliashberg equation λ for $U = 2.5$ eV, $U' = 2.0$ eV and $J = 0.25$ eV are shown in Figs. 7(a), 7(b), and 7(c), respectively. The maximum value in $\chi^{\rm sp}_{1111}$ always dominates over that of $\chi^{\rm ch}_{1212}$ and $-\chi^{\rm ch}_{1212}$, and λ does not show any enhancement.

B. Iron-based superconductor: LaFeAsO

Let us now apply multi-orbital TPSC to the iron-based superconductor, LaFeAsO. The recent discovery of high T_c superconductivity in F-doped LaFeAsO[32] has stimulated a renewed interest in multi-orbital superconductors. As for the pairing mechanism of the iron-based superconductors, several scenarios have been proposed. Among them, the possibility of the sign-reversing $s_\pm$-wave superconductivity mediated by spin fluctuations[22,33] have been extensively studied. While the $s_\pm$-wave solution has been obtained in the RPA[19,20,22] or FLEX[21] calculations for the five-orbital d-model, recently, it has been proposed that vertex corrections can enhance orbital fluctuations, and the s_{++}-pairing without sign reversing becomes dominant.[11] In this subsection, we discuss how vertex corrections in TPSC affects superconductivity in the five-orbital d-model for LaFeAsO.

The band structure of the d-model is shown in Fig. 8. The bare coupling constants are set to be $U = 1.5$ eV, $U' = 1.2$ eV, and $J = 0.15$ eV.[34] The number of electrons n is 6.1. We employ 64×64 k-point meshes and 2048 Matsubara frequencies. Hereafter orbitals 1, 2, 3, 4, and 5 denote the $d_{3z^2-r^2}$, d_{xz}, d_{yz}, $d_{x^2-y^2}$, and d_{xy} orbitals, respectively.

To see that TPSC can give enhanced orbital fluctuations, we plot $\chi^{\rm sp}_{2222}(\mathbf{q}, \omega = 0)$ and $\chi^{\rm ch}_{2424}(\mathbf{q}, \omega = 0)$ at $T = 0.015$ eV in Figs. 9(a) and 9(b), respectively. Clearly, both susceptibilities have peaks around $(\pi, 0)$ and $(0, \pi)$, and the peak in the orbital susceptibility is higher than that of the spin susceptibility. Temperature dependence of these peaks are shown in Fig. 10. We see that the peak of $\chi^{\rm ch}_{2424}(\mathbf{q}, \omega = 0)$ is more drastically enhanced
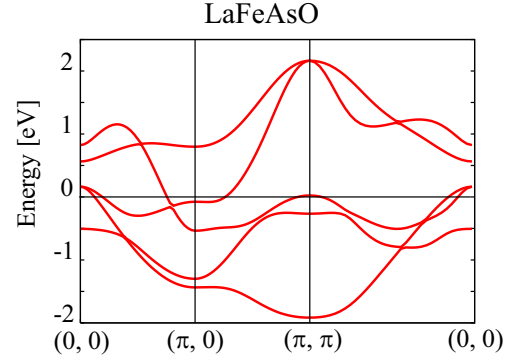

FIG. 8: (Color online) Band structure of the five-orbital d-model for LaFeAsO. The Fermi level is set at 0 eV.

than that of $\chi^{\rm sp}_{2222}(\mathbf{q}, \omega = 0)$ for $T > 0.01$ eV. While $\chi^{\rm ch}_{2424}(\mathbf{q}, \omega = 0)$ has a broad maximum peak around $T = 0.01$ eV, $\chi^{\rm sp}_{2222}(\mathbf{q}, \omega = 0)$ grows monotonously as temperature lowers.

The enhancement in the orbital susceptibility comes from the vertex correction in the charge susceptibility. To make this point clear, in Fig. 11, we plot temperature dependence of the maximum value in $\chi^{\rm ch}_{2424}(\mathbf{q}, \omega = 0)$ and $\chi^{\rm sp}_{2222}(\mathbf{q}, \omega = 0)$ obtained by RPA, for which the bare coupling constants are set to be $U = 1.2$ eV, $U' = 0.96$ eV, and $J = 0.12$ eV. We see that while $\chi^{\rm sp}_{2222}(\mathbf{q}, \omega = 0)$ diverges around $T = 0.01$ eV, $\chi^{\rm ch}_{2424}(\mathbf{q}, \omega = 0)$ has no significant temperature dependence.

In Fig. 12, we show temperature dependence of the maximum eigenvalue of the Eliashberg equation. We see that the system has a superconducting transition around $T \sim 0.005$ eV.

The associated eigenfunctions of the Eliashberg equation at $T = 0.015$ eV (the gap functions) are shown in Fig. 13 for the three bands crossing the Fermi level. We see that these gap functions have the $s_\pm$ symmetry, indicating that the spin fluctuation is the primary glue of superconductivity. However, there is a notable difference between TPSC and RPA results in the amplitudes of the gap functions on the Fermi surface. As we can see in Fig. 14, the gap amplitude is larger for
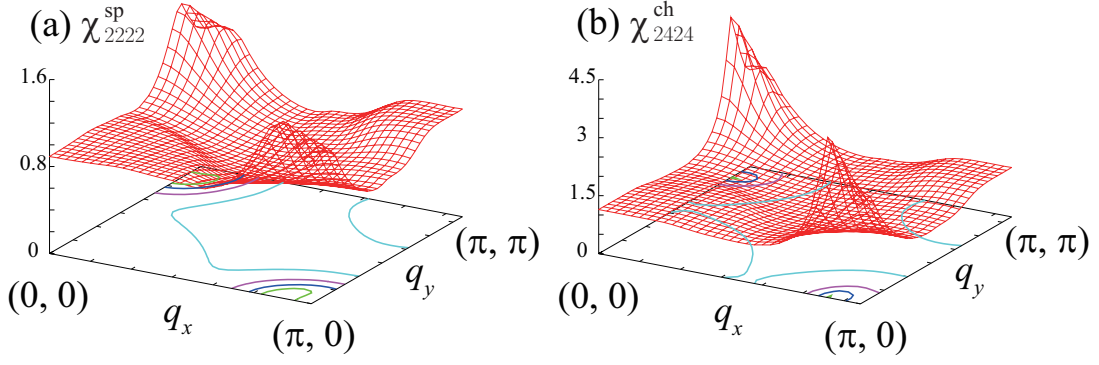
FIG. 9: (Color online) (a) $\chi_{2222}^{\text{sp}}(\mathbf{q}, \omega = 0)$ and (b) $\chi_{2424}^{\text{ch}}(\mathbf{q}, \omega = 0)$ at $T = 0.015$ eV, where orbitals 2 and 4 denote the d_{xz} and $d_{x^2-y^2}$ orbitals, respectively.
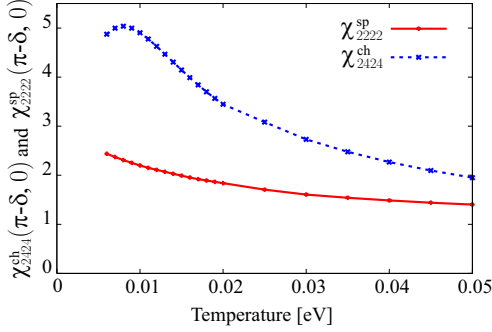

FIG. 10: (Color online) Temperature dependence of the maximum value in χ_{2222}^{sp} (red solid line) and χ_{2424}^{ch} (blue dotted line) obtained by TPSC.
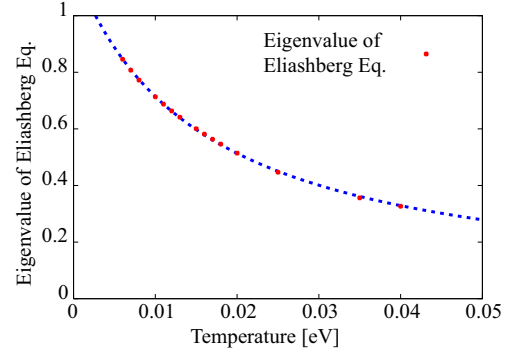

FIG. 12: (Color online) Temperature dependence of the maximum eigenvalue of the linearized Eliashberg equation. The blue dotted line is a guide to the eye.

$\mathbf{V}(k) = -\frac{3}{2}\mathbf{U}^{\text{sp}}\boldsymbol{\chi}^{\text{sp}}(k)\,\mathbf{U}_0^{\text{sp}}$ in the Eliashberg equation, then we find that the gap amplitude becomes large on the Fermi surface as in the RPA result [see Fig. 14(d)].

IV. SUMMARY

To summarize, we have developed the two-particle self consistent method (TPSC) for the multi-orbital Hubbard model. We derived self-consistent equations to determine vertex corrections in the spin and charge (orbital) susceptibilities. We applied this method to the effective models for La$_2$CuO$_4$ and LaFeAsO. We solved the linearized Eliashberg equation and found that vertex corrections play a crucial role in the multi-orbital superconductors.

In the two-orbital $d_{x^2-y^2}$-$d_{3z^2-r^2}$ model for La$_2$CuO$_4$, while FLEX shows much lower T_c than its experimental value ~ 40 K, the present TPSC can increase T_c dramatically due to enhanced orbital fluctuations via vertex corrections for intermediate $U \sim 2.0$ eV.

In the iron-based superconductor LaFeAsO, we have studied whether orbital fluctuations can be enhanced and

FIG. 11: (Color online) Temperature dependence of the maximum value in χ_{2222}^{sp} (red solid line) and χ_{2424}^{ch} (blue dotted line) obtained by RPA. The bare coupling constants are set to be $U = 1.2$ eV, $U' = 0.96$ eV, and $J = 0.12$ eV.

RPA than TPSC. This indicates that there is a frustration between the orbital-fluctuation-mediated pairing and the spin-fluctuation-mediated pairing. Indeed, in TPSC, if we drop the contribution of the charge channel in the pairing interaction, namely consider only
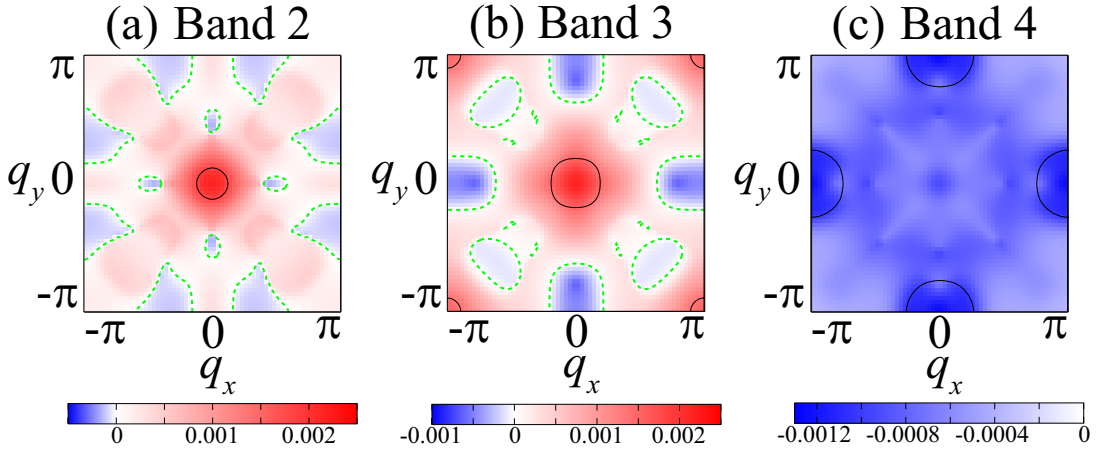
FIG. 13: (Color online) Gap functions obtained by TPSC for the bands with the (a) second, (b) third, and (c) fourth Kohn-Sham energy at $T = 0.015$ eV. The black line and dotted green line represent the Fermi surface and nodes of gap functions, respectively.
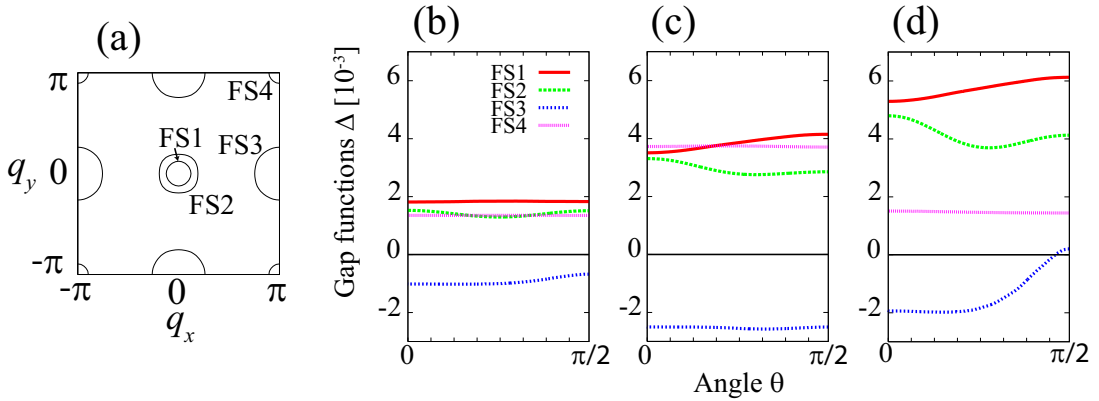

FIG. 14: (Color online) Gap function on the (a) Fermi surfaces by (b) TPSC, (c) RPA, and (d) TPSC without charge fluctuation, where θ is the rotation angle from the k_y axis.

induce the s_{++}-wave pairing within TPSC. Indeed we have found that some kinds of orbital fluctuations are enhanced by considering vertex correction and become even stronger than spin fluctuations. However, their orbital fluctuations are not strong enough to cause the s_{++}-wave pairing, and the obtained gap function has the $s_{\pm}$ symmetry, although the gap magnitude is relatively suppressed due to a frustration between two kinds of pairing interactions mediated by spin and orbital fluctuations. It is an interesting problem in future research whether the pairing symmetry changes for larger interaction parameters. Another important future issue is a systematic comparison between the present multi-orbital TPSC and other (diagrammatic) methods which consider the vertex corrections. Finally, we stress the importance of vertex corrections in multi-orbital systems for cooperative and competitive phenomena between spin and orbital degrees of freedoms.

Appendix A: Definition of correlation functions

In the single-orbital case, correlation functions for spin $S^z(\mathbf{r})$ and charge $n(\mathbf{r})$ are defined as

$$\chi^{\text{sp}}(1,2) = \langle T_\tau S^z(1)S^z(2)\rangle, \tag{A1a}$$

$$\chi^{\text{ch}}(1,2) = \langle T_\tau n(1)n(2)\rangle - \langle n(1)\rangle\langle n(2)\rangle, \tag{A1b}$$

where an abbreviation $1 = (\mathbf{r}_1, \tau_1)$ denotes a position $\mathbf{r}_1$ and an imaginary time τ_1, and T_τ is the time ordering operator. Time dependence of a generic operator $Q(\mathbf{r})$ is defined as $Q(\mathbf{r},\tau) = e^{-\tau H}Q(\mathbf{r})e^{\tau H}$. $\chi^{\text{sp(ch)}}(q)$ in the main text is the Fourier transform of the above real-space representation. The two sum rules (Eqs. (2)), which play a central role in TPSC, originate from the definition at equal time, that is, $\chi^{\text{sp(ch)}}(1,1^+)$ with $1^+ = (\mathbf{r}_1, \tau_1 + \delta)$

$(\delta > 0)$.

In the multi-orbital case, we consider correlation functions for $\mathbf{S}_{\mu\nu}(1) = (c^\dagger_{\mu\uparrow}(1), c^\dagger_{\nu\downarrow}(1))\,\boldsymbol{\sigma}\,(c_{\mu\uparrow}(1), c_{\nu\downarrow}(1))^T$, and $n_{\mu\nu}(1) = c^\dagger_{\mu\uparrow}(1)c_{\nu\uparrow}(1) + c^\dagger_{\mu\downarrow}(1)c_{\nu\downarrow}(1)$. These correlation functions for spin and charge channels are defined as

$$\chi^{\text{sp}z}_{\lambda\mu\nu\xi}(1,2) = \langle T_\tau S^z{}_{\lambda\mu}(1)S^z{}_{\xi\nu}(2)\rangle, \tag{A2a}$$

$$\chi^{\text{sp}\pm}_{\lambda\mu\nu\xi}(1,2) = \langle T_\tau S^+{}_{\lambda\mu}(1)S^-{}_{\xi\nu}(2)\rangle, \tag{A2b}$$

$$\chi^{\text{ch}}_{\lambda\mu\nu\xi}(1,2) = \langle T_\tau n_{\lambda\mu}(1)n_{\xi\nu}(2)\rangle - \langle n_{\lambda\mu}(1)\rangle\langle n_{\xi\nu}(2)\rangle. \tag{A2c}$$

The sum rules of Eqs. (8) and (9) come from the following definitions at equal time,

$$\chi^{\text{sp}z}_{\lambda\mu\nu\xi}(1,1^+) = \langle(c^\dagger_{\lambda\uparrow}(1)c_{\mu\uparrow}(1) - c^\dagger_{\lambda\downarrow}(1)c_{\mu\downarrow}(1))(c^\dagger_{\xi\uparrow}(1^+)c_{\nu\uparrow}(1^+) - c^\dagger_{\xi\downarrow}(1^+)c_{\nu\downarrow}(1^+))\rangle \\ - \langle(c^\dagger_{\lambda\uparrow}(1)c_{\mu\uparrow}(1) - c^\dagger_{\lambda\downarrow}(1)c_{\mu\downarrow}(1))\rangle\langle(c^\dagger_{\xi\uparrow}(1^+)c_{\nu\uparrow}(1^+) - c^\dagger_{\xi\downarrow}(1^+)c_{\nu\downarrow}(1^+))\rangle \tag{A3a}$$

$$\chi^{\text{sp}\pm}_{\lambda\mu\nu\xi}(1,1^+) = 2\langle c^\dagger_{\lambda\uparrow}(1)c_{\mu\downarrow}(1)c^\dagger_{\xi\downarrow}(1^+)c_{\nu\uparrow}(1^+)\rangle \tag{A3b}$$

$$\chi^{\text{ch}}_{\lambda\mu\nu\xi}(1,1^+) = \langle(c^\dagger_{\lambda\uparrow}(1)c_{\mu\uparrow}(1) + c^\dagger_{\lambda\downarrow}(1)c_{\mu\downarrow})(c^\dagger_{\xi\uparrow}(1^+)c_{\nu\uparrow}(1^+) + c^\dagger_{\xi\downarrow}(1^+)c_{\nu\downarrow}(1^+))\rangle \\ - \langle(c^\dagger_{\lambda\uparrow}(1)c_{\mu\uparrow}(1) + c^\dagger_{\lambda\downarrow}(1)c_{\mu\downarrow})(c^\dagger_{\xi\uparrow}(1^+)c_{\nu\uparrow}(1^+) + c^\dagger_{\xi\downarrow}(1^+)c_{\nu\downarrow}(1^+))\rangle. \tag{A3c}$$

Appendix B: Ansatz for effective interactions in single-orbital case

Following Vilk and Tremblay,[17] let us derive the ansatz, Eq. (4), used in TPSC calculations. The four-point vertex function, $\Gamma_{\sigma\sigma'}$, between electrons with spin σ and σ' is given by

$$\Gamma_{\sigma\sigma'}\delta(1-3)\delta(2-4)\delta(2-1^+) = \frac{\delta\Sigma_\sigma(1,2)}{\delta G_{\sigma'}(3,4)}, \tag{B1}$$

where $G_\sigma(1,2)$ and $\Sigma_\sigma(1,2)$ is the dressed Green's function and self energy with spin σ. The equation of motion and the Dyson equation leads to the relation,

$$\Sigma_\sigma(1,\bar{1})G_\sigma(\bar{1},2) \\ = -U\langle T_\tau[c^\dagger_{\bar{\sigma}}(1^{++})c_{\bar{\sigma}}(1^+)c_\sigma(1)c^\dagger_\sigma(2)]\rangle, \tag{B2}$$

with $\bar{\sigma} = -\sigma$. Here a bar over a number means the integral over position and imaginary time. The four-point correlation function can be approximated by the local correlation function and the Green's function as follows,

$$- U\langle T_\tau[c^\dagger_{\bar{\sigma}}(1^{++})c_{\bar{\sigma}}(1^+)c_\sigma(1)c^\dagger_\sigma(2)]\rangle \\ \sim U\frac{\langle n_\uparrow(1)n_\downarrow(1)\rangle}{\langle n_\uparrow(1)\rangle\langle n_\downarrow(1)\rangle}G_{\bar{\sigma}}(1,1^+)G_\sigma(1,2). \tag{B3}$$

By substituting Eq. (B3) into Eq. (B1), we can obtain

$$\Gamma_{\sigma\sigma'}\delta(1-3)\delta(2-4)\delta(2-1^+) = \frac{\delta\Sigma_\sigma(1,2)}{\delta G_{\sigma'}(3,4)} = \frac{\delta\left[U\frac{\langle n_\uparrow n_\downarrow\rangle}{\langle n_\uparrow\rangle\langle n_\downarrow\rangle}G_{\bar{\sigma}}(1,1^+)\delta(1-2)\right]}{\delta G_{\sigma'}(3,4)} \\ = \frac{\delta\left[U\frac{\langle n_\uparrow n_\downarrow\rangle}{\langle n_\uparrow\rangle\langle n_\downarrow\rangle}\right]}{\delta G_{\sigma'}(3,4)}G_{\bar{\sigma}}(1,1^+)\delta(1-2) + U\frac{\langle n_\uparrow n_\downarrow\rangle}{\langle n_\uparrow\rangle\langle n_\downarrow\rangle}\frac{\delta G_{\bar{\sigma}}(1,1^+)}{\delta G_{\sigma'}(3,4)}\delta(1-2). \tag{B4}$$

The last term of this equation is proportional to $\delta_{\bar{\sigma}\sigma'}$ via

$$\frac{\delta G_{\bar{\sigma}}(1,1^+)}{\delta G_{\sigma'}(3,4)} = \delta_{\bar{\sigma}\sigma'}\delta(1-3)\delta(4-1^+), \tag{B5}$$

and then contributes to the spin channel, $U_{\text{sp}} = \Gamma_{\sigma\bar{\sigma}} - \Gamma_{\sigma\sigma}$. This just provides Eq. (4) for U_{sp}.

Appendix C: Ansatz in multi-orbital systems

In this section, let us extend the above-mentioned ansatz into the multi-orbital case. In this case, the four-point vertex function has orbital indices, λ, μ, ν, ξ besides spin index, σ. We here consider $\Gamma_{(\mu\mu\sigma)(\nu\nu\sigma')}$, which can be written by only orbital-diagonal components.

$$\Gamma_{(\mu\mu\sigma)(\nu\nu\sigma')}\delta(1-3)\delta(2-4)\delta(2-1^+) = \frac{\delta\Sigma_{\mu\mu\sigma}(1,2)}{\delta G_{\nu\nu\sigma'}(3,4)} = \frac{\delta\left[\Sigma_{\mu\mu\sigma}(1,\bar{5})[\mathbf{G}(\bar{5},\bar{6})\mathbf{G}^{-1}(\bar{6},2)]_{\mu\mu\sigma}\right]}{\delta G_{\nu\nu\sigma'}(3,4)}$$

$$\sim \frac{\delta}{\delta G_{\nu\nu\sigma'}(3,4)}\left(-U\frac{\langle n_{\mu\sigma}n_{\mu\bar{\sigma}}\rangle}{\langle n_{\mu\sigma}\rangle\langle n_{\mu\bar{\sigma}}\rangle}G_{\mu\mu\bar{\sigma}}(1,1^+) - \sum_{\xi\neq\mu}U'\frac{\langle n_{\mu\sigma}n_{\xi\bar{\sigma}}\rangle}{\langle n_{\mu\sigma}\rangle\langle n_{\xi\bar{\sigma}}\rangle}G_{\xi\xi\bar{\sigma}}(1,1^+) - \sum_{\xi\neq\mu}(U'-J)\frac{\langle n_{\mu\sigma}n_{\xi\sigma}\rangle}{\langle n_{\mu\sigma}\rangle\langle n_{\xi\sigma}\rangle}G_{\xi\xi\sigma}(1,1^+)\right)$$

$$\sim -U\frac{\langle n_{\mu\sigma}n_{\mu\bar{\sigma}}\rangle}{\langle n_{\mu\sigma}\rangle\langle n_{\mu\bar{\sigma}}\rangle}\frac{\delta G_{\mu\mu\bar{\sigma}}(1,1^+)}{\delta G_{\nu\nu\sigma'}(3,4)} - \sum_{\xi\neq\mu}U'\frac{\langle n_{\mu\sigma}n_{\xi\bar{\sigma}}\rangle}{\langle n_{\mu\sigma}\rangle\langle n_{\xi\bar{\sigma}}\rangle}\frac{\delta G_{\xi\xi\bar{\sigma}}(1,1^+)}{\delta G_{\nu\nu\sigma'}(3,4)} - \sum_{\xi\neq\mu}(U'-J)\frac{\langle n_{\mu\sigma}n_{\xi\sigma}\rangle}{\langle n_{\mu\sigma}\rangle\langle n_{\xi\sigma}\rangle}\frac{\delta G_{\xi\xi\sigma}(1,1^+)}{\delta G_{\nu\nu\sigma'}(3,4)}. \tag{C1}$$

Here, following the single-orbital case, we have introduced the following approximations,

$$\Sigma_{\mu\mu\sigma}G_{\mu\mu\sigma}G_{\mu\mu\sigma}^{-1} \sim -U\frac{\langle n_{\mu\sigma}n_{\mu\bar{\sigma}}\rangle}{\langle n_{\mu\sigma}\rangle\langle n_{\mu\bar{\sigma}}\rangle}G_{\mu\mu\bar{\sigma}}(1,1^+),$$

$$\Sigma_{\mu\mu\sigma}G_{\xi\xi\sigma}G_{\xi\xi\sigma}^{-1} \sim -U'\frac{\langle n_{\mu\sigma}n_{\xi\sigma}\rangle}{\langle n_{\mu\sigma}\rangle\langle n_{\xi\bar{\sigma}}\rangle}G_{\xi\xi\bar{\sigma}}(1,1^+),$$

$$\Sigma_{\mu\mu\sigma}G_{\xi\xi\bar{\sigma}}G_{\xi\xi\bar{\sigma}}^{-1} \sim -U'\frac{\langle n_{\mu\sigma}n_{\xi\bar{\sigma}}\rangle}{\langle n_{\mu\sigma}\rangle\langle n_{\xi\bar{\sigma}}\rangle}G_{\xi\xi\bar{\sigma}}(1,1^+).$$

Eq. (10a) for $U_{\mu\mu\mu\mu}^{\rm sp}$ can be obtained from the first term of Eq. (C1), since the intra-orbital Coulomb interaction for the orbital μ is proportional to $\delta_{\mu\mu}\delta_{\sigma\bar{\sigma}}$. In the same way, Eq. (10b) for $U_{\mu\nu\mu\nu}^{\rm sp}$ and Eq. (10c) for $U_{\mu\nu\mu\nu}^{\rm sp} - J^{\rm sp}$ with $\mu \neq \nu$ can be obtained from the second and the third terms in Eq. (C1), respectively.

[1] H. Suhl, B.T. Matthias, L.R. Walker, Phys. Rev. Lett., **3** 552 (1959)

[2] J. Kondo, Progr. Theor. Phys., **29** 1 (1963)

[3] J. Nagamatsu, N. Nakagawa, T. Muranaka, Y. Zenitani and J. Akimitsu, Nature (London) **410** 63 (2001).

[4] For review, see, e.g., O. Gunnarsson, Rev. Mod. Phys. **69**, 575 (1997), M. Capone, M. Fabrizio, C. Castellani, and E. Tosatti, ibid. **81**, 943 (2009).

[5] K. Takada *et al.*, Nature (London) 422, 53 (2003).

[6] For review, see, e.g., A.P. Mackenzie and Y. Maeno, Rev. Mod. Phys. 75, 657 (2003). Y. Maeno, S. Kittaka, T. Nomura, S. Yonezawa, and K. Ishida, J. Phys. Soc. Jpn, **81**, 011009 (2009).

[7] For review, see, e.g., J. Paglione and R. L. Greene, Nat. Phys. **6** 645 (2010).

[8] For review, see, e.g., C. Pfleiderer, Rev. Mod. Phys., **81** 1551 (2009).

[9] J. R. Schrieffer, *Theory of Superconductivity* (Westview Press, Colorado, 1971).

[10] M. Mochizuki, Y. Yanase and M. Ogata, Phys. Rev. Lett. **94**, 147005 (2005).

[11] H. Kontani and S. Onari, Phys. Rev. Lett. 104, 157001 (2010).

[12] D. J. Scalapino, E. Loh Jr., and J. E. Hirsch, Phys. Rev. B 34, 8190 (1986).

[13] N. E. Bickers and D. J. Scalapino: Ann. Phys. (N.Y.) 193 (1989) 206.

[14] G. Baym and L. P. Kadanoff: Phys. Rev. 124 (1961) 287, G. Baym: ibid. 127 (1962) 1391.

[15] H. Kusunose, J. Phys. Soc. Jpn. 79, 094707 (2010).

[16] S. Onari and H. Kontani, Phys. Rev. Lett. **109**, 137001 (2012).

[17] Y.M. Vilk, A.-M.S. Tremblay, J. Phys. I France 7, 1309 (1997).

[18] H. Sakakibara, H. Usui, K. Kuroki, R. Arita and H. Aoki, Phys. Rev. Lett. **105**, 057003 (2010), Phys. Rev. B **85** 064501 (2012).

[19] S. Graser, T. A. Maier, P. J. Hirschfeld, and D. J. Scalapino, New J. Phys. 11, 025016 (2009).

[20] K. Kuroki, S. Onari, R. Arita, H. Usui and H. Aoki, Phys. Rev. B **79**, 224511 (2009).

[21] H. Ikeda, J. Phys. Soc. Jpn. **77**, 123707 (2008), R. Arita and H. Ikeda, ibid. **78**, 113707 (2009), H. Ikeda, R. Arita and J. Kuneš, Phys. Rev. B **82** 024508 (2010); **81** 054502 (2010).

[22] K. Kuroki, S. Onari, R. Arita, H. Usui, H. Kontani, Y. Tanaka and H. Aoki, Phys. Rev. Lett. **101**, 087004 (2008).

[23] T. Takimoto, T. Hotta, and K. Ueda, Phys. Rev. B **69**, 104504 (2004).

[24] The Hund's coupling in the charge channel is always renormalized to be small in our case, and sometimes causes unexpected problematic behavior.

[25] N. Marzari and D. Vanderbilt, Phys. Rev. B **56**, 12847 (1997), I. Souza, N. Marzari and D. Vanderbilt, ibid. **65**,

035109 (2001).

[26] J. P. Perdew, K. Burke, M. Ernzerhof, Phys. Rev. Lett. **77**, 3865 (1996).

[27] P. Blaha *et al.*, http://www.wien2k.at.

[28] J. Kuneš, R. Arita, P. Wissgott, A.Toschi, H. Ikeda, K. Held, Comp. Phys. Commun. **181**, 1888 (2010).

[29] A. A. Mostofi, J. R. Yates, Y.-S. Lee, I. Souza, D. Vanderbilt and N. Marzari, Comput. Phys. Commun. **178**, 685 (2008).

[30] The filling n of the lower band composed mainly of the $d_{3z^2-r^2}$ orbital is approximately 1.90. According to Ref.17, to fit the idea of the approximation for the electron gas proposed by Singwi *et al.*,[31] the electron-hole transformation should be applied on the $d_{3z^2-r^2}$ orbital. We confirmed that the numerical results shown in this section does not change under the electron-hole transformation for the $d_{3z^2-r^2}$ orbital.

[31] For a review, see K. S. Singwi and M. P. Tosi, in Solid State Physics, edited by H. Ehrenreich, F. Seitz, and D. Turnbull (Academic, New York, 1981), Vol. 36, p. 177; S. Ichimaru, Rev. Mod. Phys. 54, 1017 (1982).

[32] Y. Kamihara *et al.*, J. Am. Chem. Soc. 130, 3296 (2008)

[33] I. I. Mazin, D. J. Singh, M. D. johannes, and M. H. Du, Phys. Rev. Lett. 101, 057003 (2008)

[34] Even if we change the values of these interaction parameters by 10 %, the qualitative tendency of the present result does not change.